

Supporting information for

3D local earthquake tomography of the Ecuadorian margin in the source area of the 2016 Mw 7.8 Pedernales earthquake

Sergio León-Ríos^{1*}, Lidong Bie¹, Hans Agurto-Detzel², Andreas Rietbrock¹, Audrey Galve², Alexandra Alvarado³, Susan Beck⁴, Philippe Charvis², Yvonne Font², Silvana Hidalgo³, Mariah Hoskins⁵, Mireille Laigle², Davide Oregioni², Anne Meltzer⁵, Mario Ruiz³ and Jack Wollam¹

1. Karlsruhe Institute of Technology, Geophysical Institute, Karlsruhe, 76187, Germany
2. Université Côte d'Azur, IRD, CNRS, Observatoire de la Côte d'Azur, Géoazur, 06304, Nice, France
3. Instituto Geofísico, Escuela Politécnica Nacional, Quito, 170525, Ecuador
4. Department of Geosciences, University of Arizona, Tucson, AZ 95721, USA
5. Department of Earth and Environmental Sciences, Lehigh University, Bethlehem, PA 18015, USA

Contents of this file

- Supporting Information 1: Inversion grid.
- Supporting Information 2: Damping curves.
- Supporting Information 3: MRM analysis.
- Supporting Information 4: Checkerboard test.
- Supporting Information 5: Synthetic model. Testing anomalies on Vp model.
- Supporting Information 6: Synthetic model. Testing influence of 2D initial model.
- Supporting Information 7: 3D velocity model, merging modeling strategy. Horizontal slices.
- Supporting Information 8: 3D velocity model, merging modeling strategy. Cross sections.
- Supporting Information 9: Estimated standard deviation.
- Supporting Information 10: Analyzing Vp iso-velocity contours.
- Supporting Information 11: Constrasting residual bathymetry and Vp horizontal slice.
- Supporting Information 12: MRM analysis along strike.

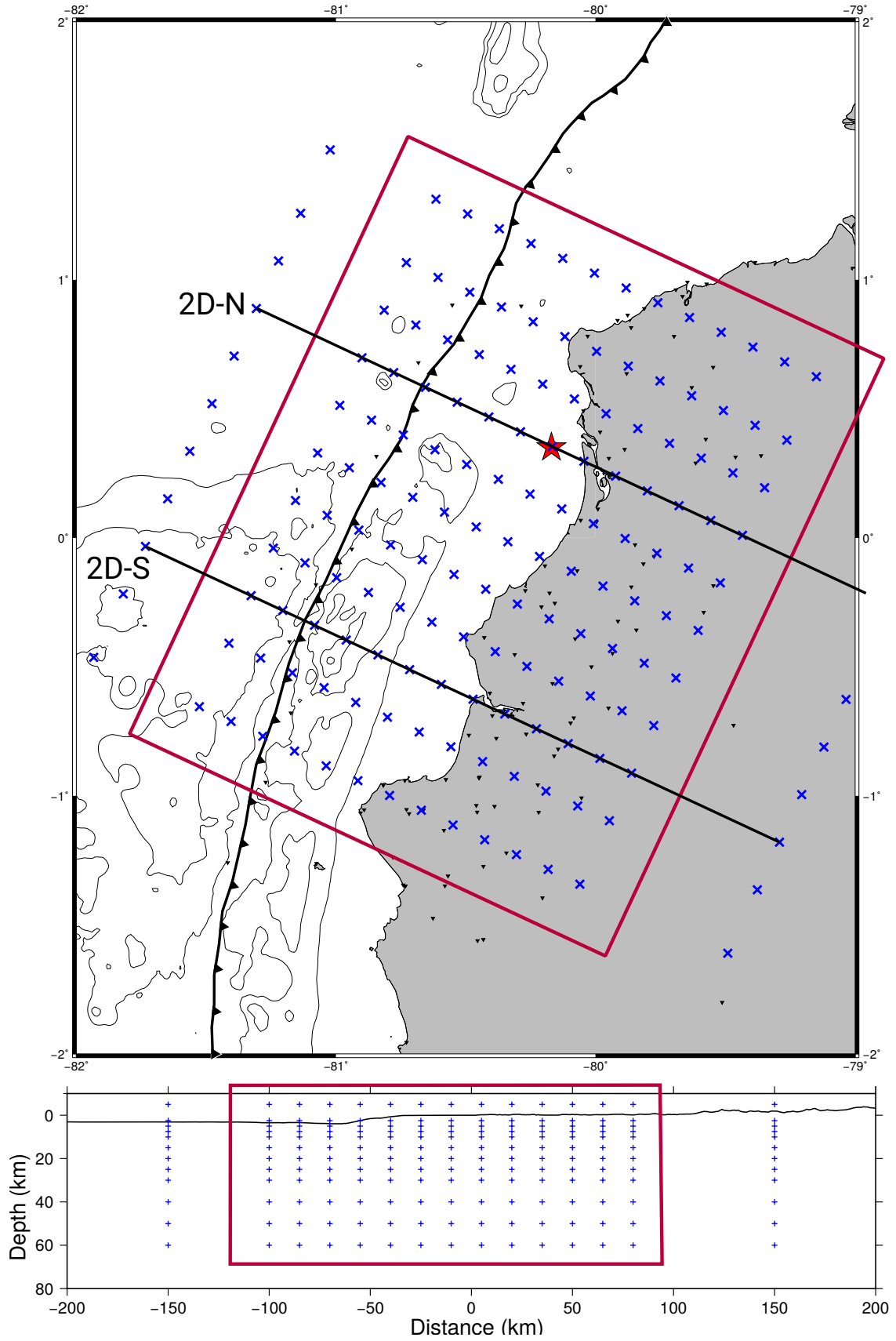


Figure S 1: Grid nodes distribution for the inversion process. Outer rectangle shows the distribution for the coarse grid, while inner rectangle represents the fine grid with a 15 km W-E nodes spacing and 22.5 km separation along strike. Bottom image shows the distribution in depth following the layering of the minimum 1D velocity model (Leon-Rios et al., 2019).

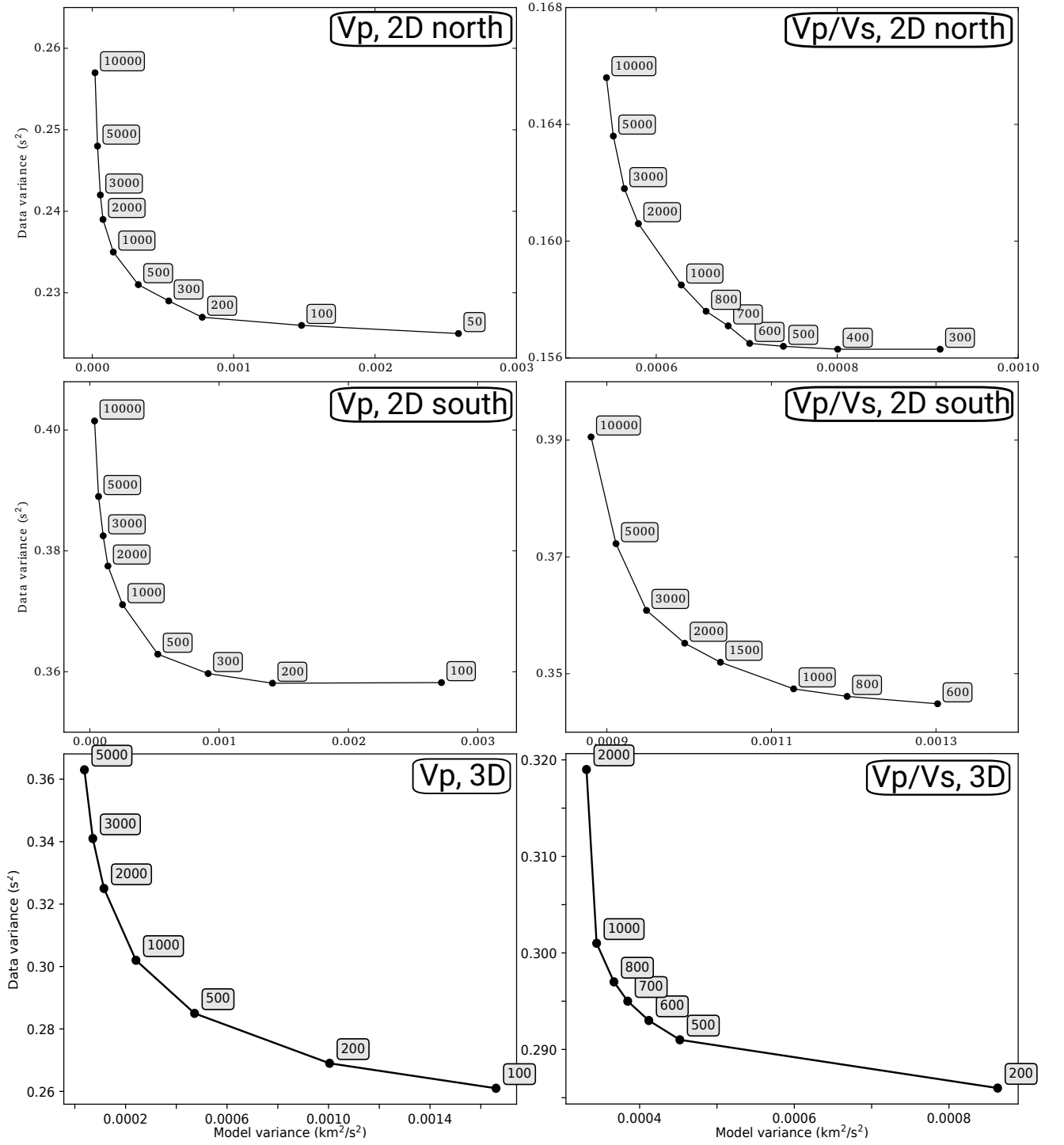


Figure S 2: Damping curves. Trade-off curves analysis for the different stages of this work. Left side shows the Vp and right side the Vp/Vs ratio. Damping curves were calculated for north and south segments in the 2D inversion, and for the complete dataset in the 3D inversion stage.

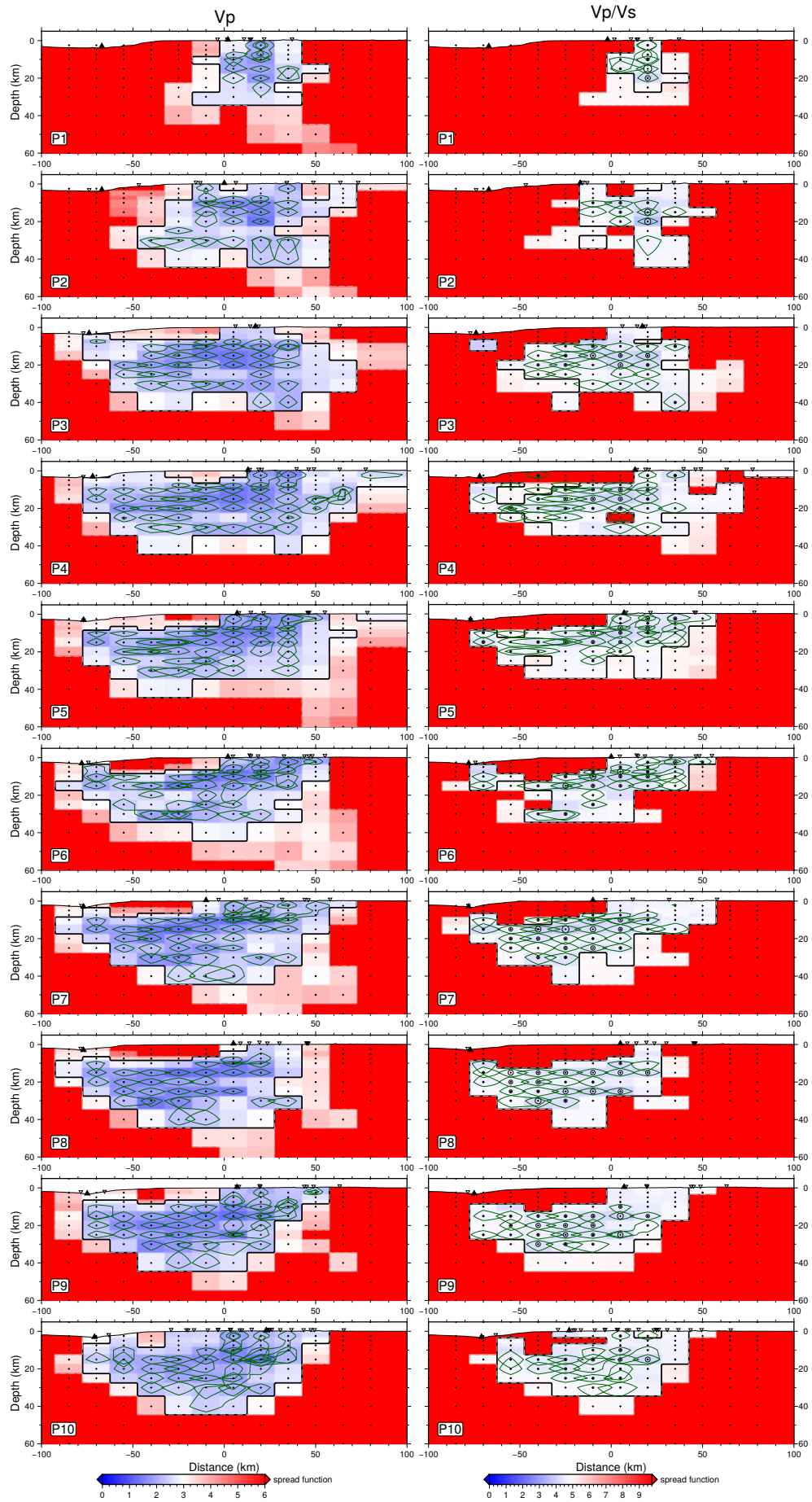
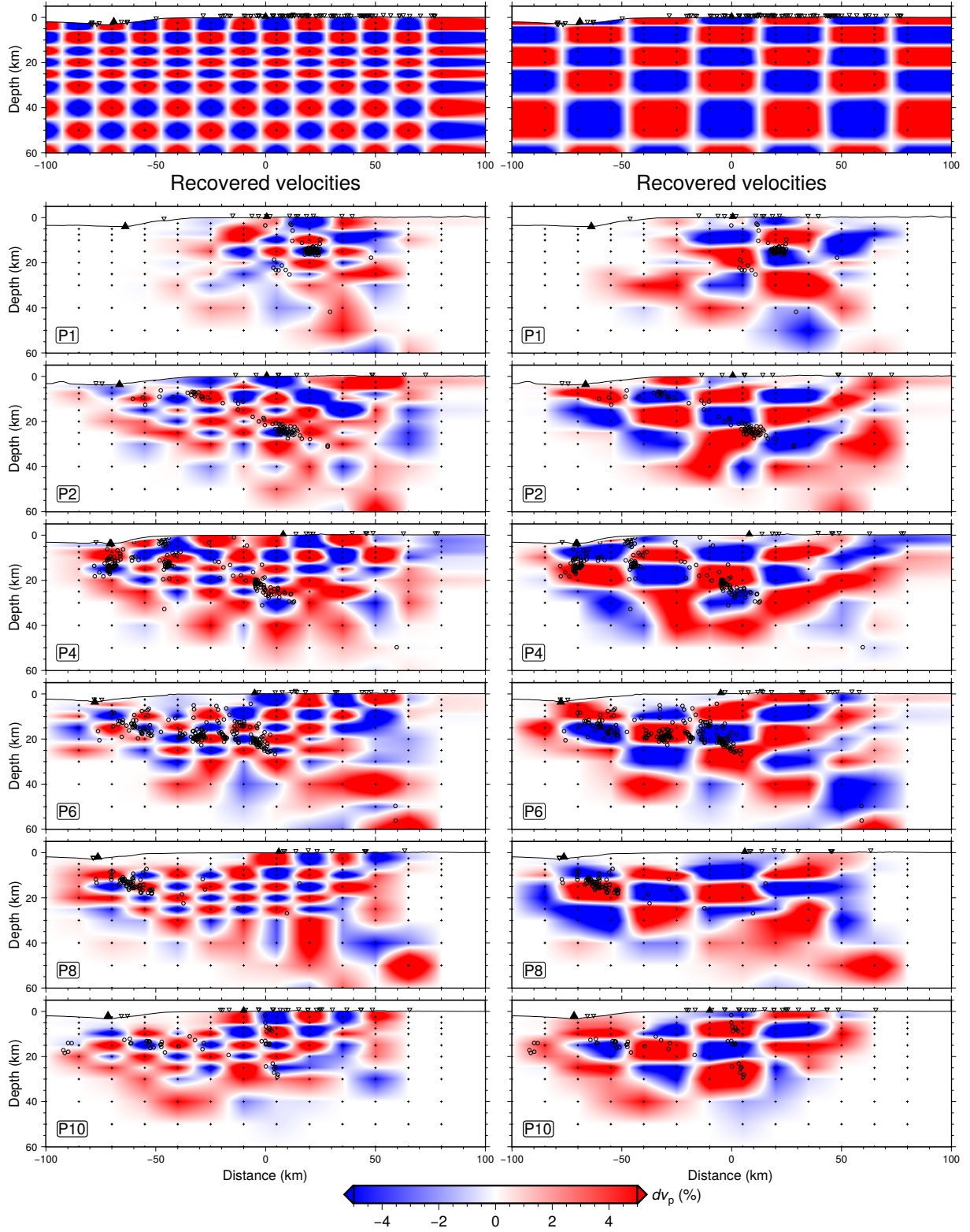


Figure S 3: MRM analysis. Model resolution matrix analysis using the spread function and the 70% of the diagonal elements of the MRM. Spread function is color coded with a blue-red with blue colors representing well resolved regions.



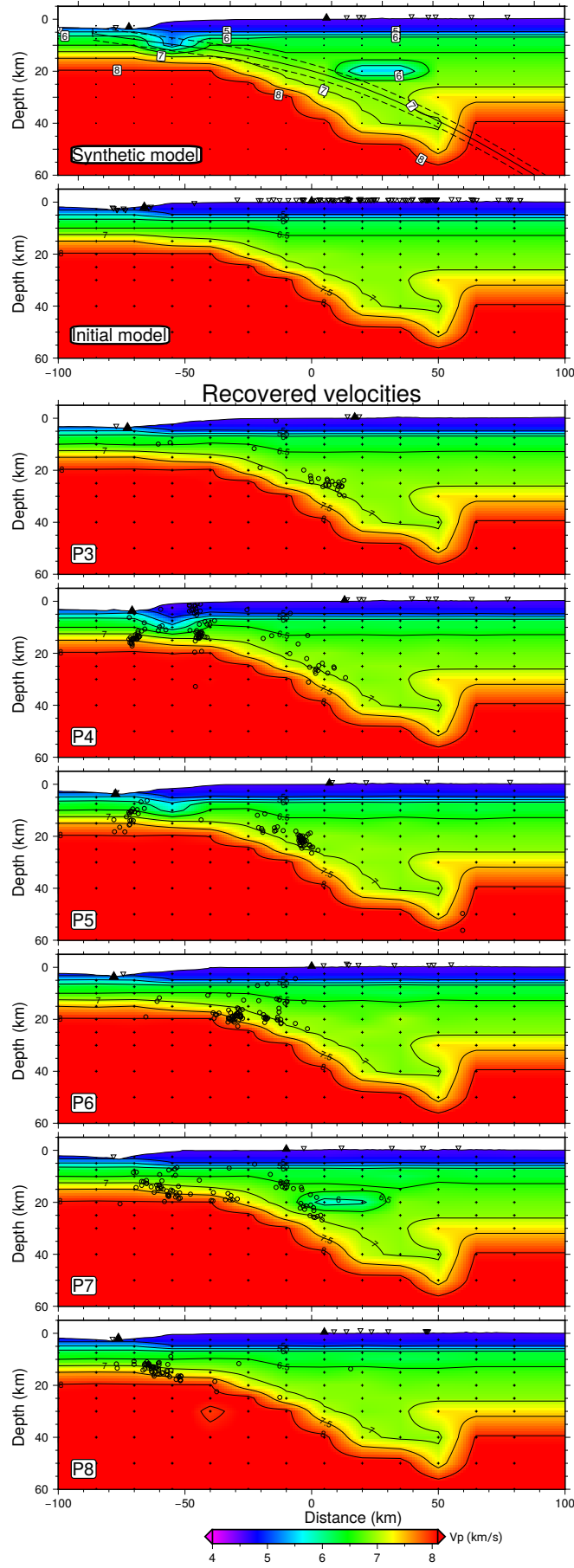


Figure S 5: Synthetic recovery test for a seamount represented by low V_p anomalies added in P4-P5. Also, a low velocity anomaly was included at 20 km depth in P7. Projection of the input model is shown at the top.

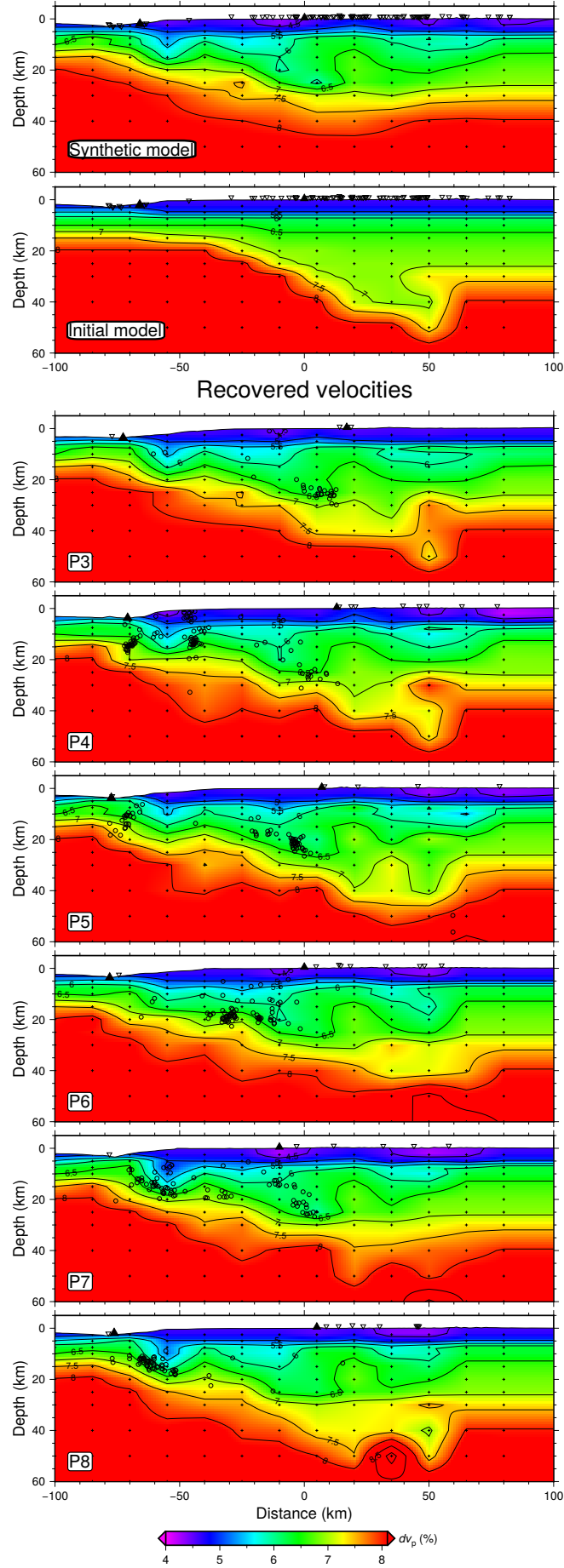


Figure S 6: Synthetic restoring test to evaluate the influence of our 2D V_p northern segment model (2D-N), over a homogeneous subduction zone. Synthetic arrival times were generated using the synthetic model (2D-N) and then tested over the homogeneous initial model. Recovered velocities are shown for central profiles (P3-P8).

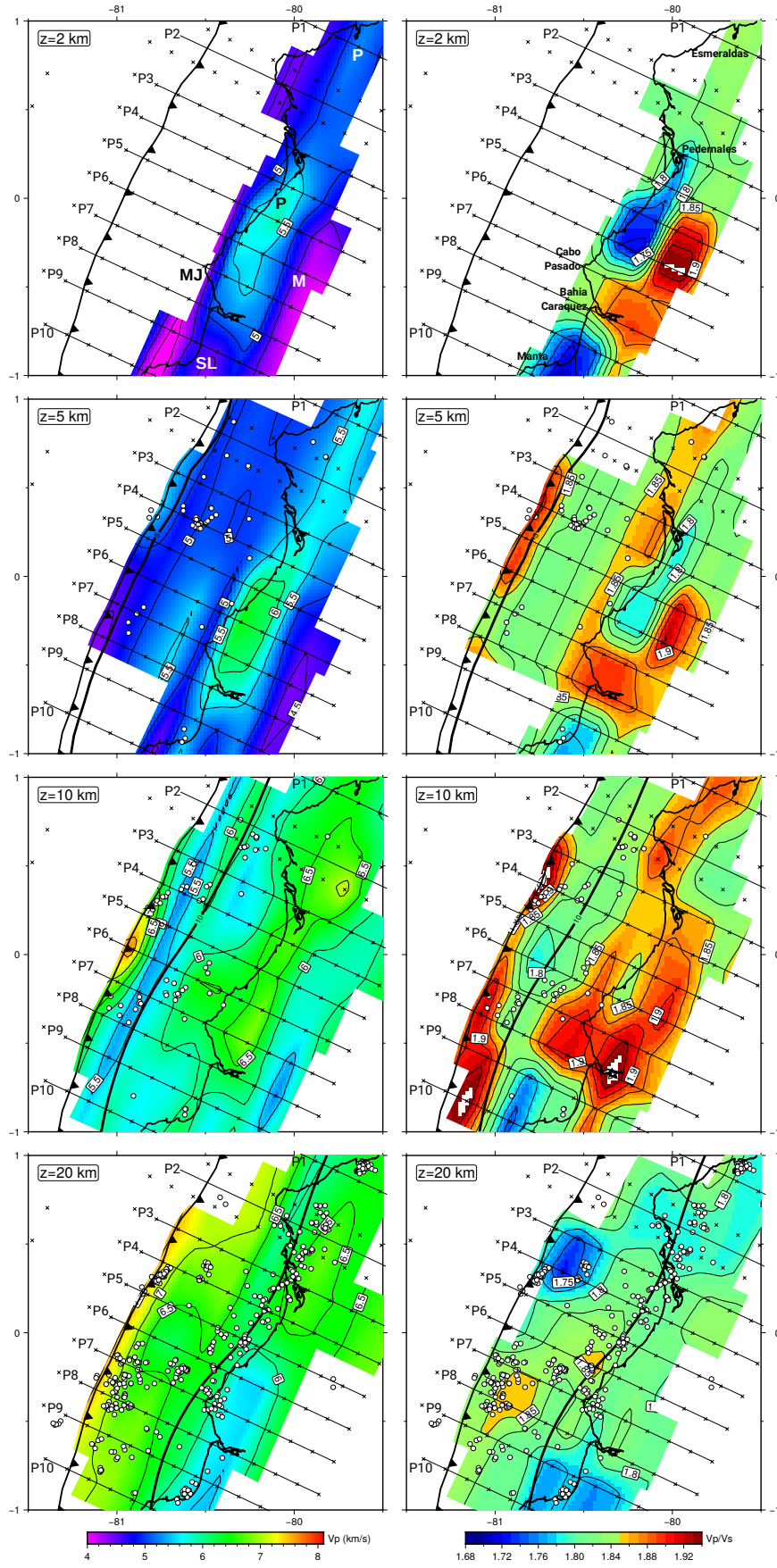


Figure S 7: 3D velocity model, merging modeling strategy. Horizontal slices. V_p (left) and V_p/V_s (right) horizontal slices at 2, 5, 10 and 20 km depth. Velocities and V_p/V_s ratios are color coded and iso-contours are plotted every 1.0 km/s and 0.025 for V_p and V_p/V_s , respectively. Based on MRM and checkerboard test, non resolved areas are blank. Seismicity is plotted by depth (d) following: $d \leq 5$ km in $z=5$ km, $5 < d \leq 10$ km in $z=10$ km and $d > 10$ km in $z=20$ km. Further details in Figure 6 in main text.

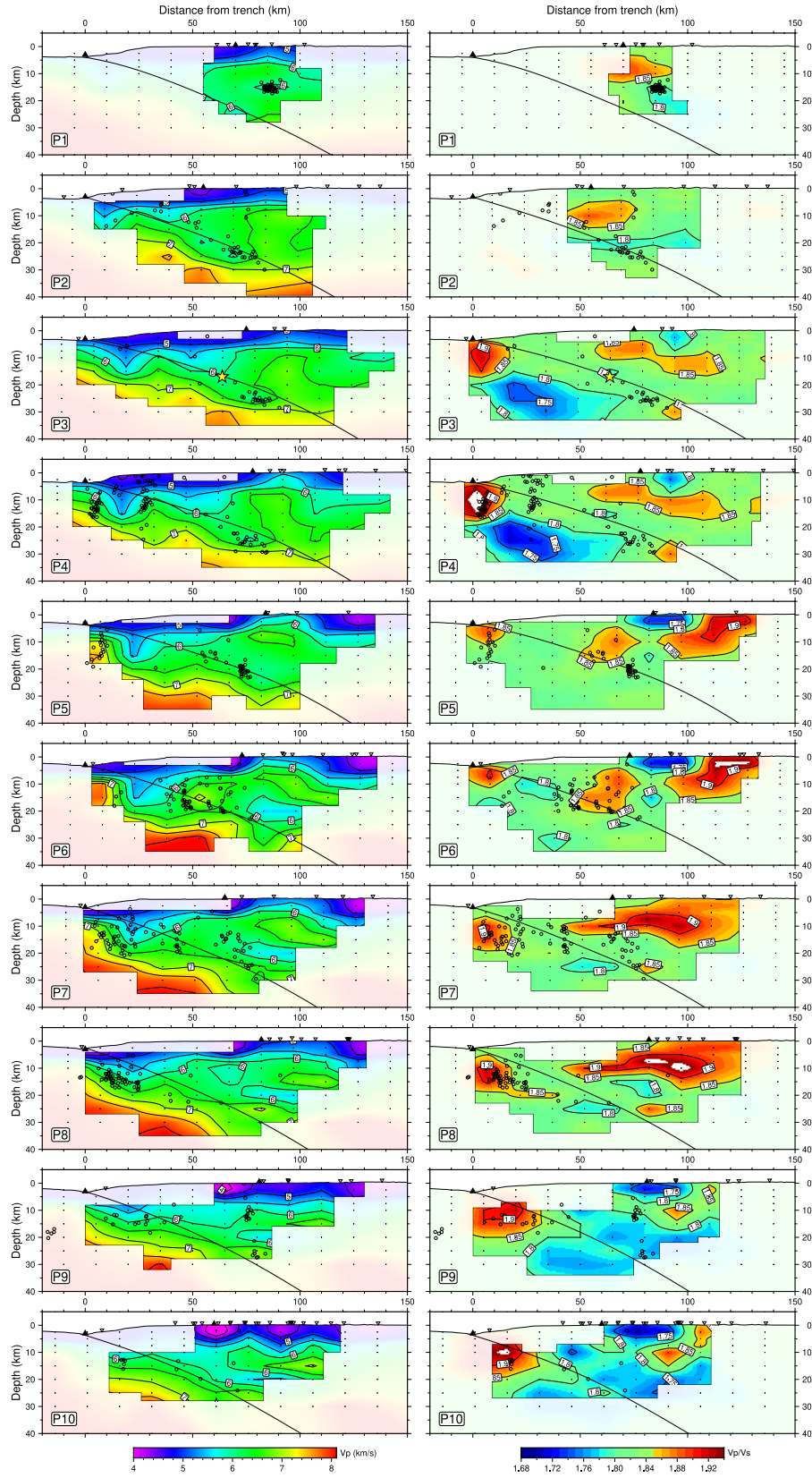


Figure S 8: 3D velocity model, merging modeling strategy. Cross sections. Three-dimensional models for both V_p (left) and V_p/V_s (right) based on a 2D-N and 2D-S merged initial model. Results are shown along 10 W-E profiles. V_p velocities and V_p/V_s ratios are color coded and iso-contours are plotted every 1.0 km/s and 0.025 for V_p and V_p/V_s , respectively. Based on the MRM and checkerboard test, non resolved areas are faded. Location of profiles, P1-P10, is shown in Figure 1. Width for projection of hypocenters and stations is 22 km. Relocated hypocenters are plotted in black circles, and stations are represented by inverted triangles. Grid nodes are displayed in black crosses and solid black triangles represent the projection of the trench and coastline. Yellow star in P3 indicates the hypocenter for the 2016 Pedernales earthquake (Nocquet et al., 2017). Modified slab interface (see main text for further details) is represented by solid black line.

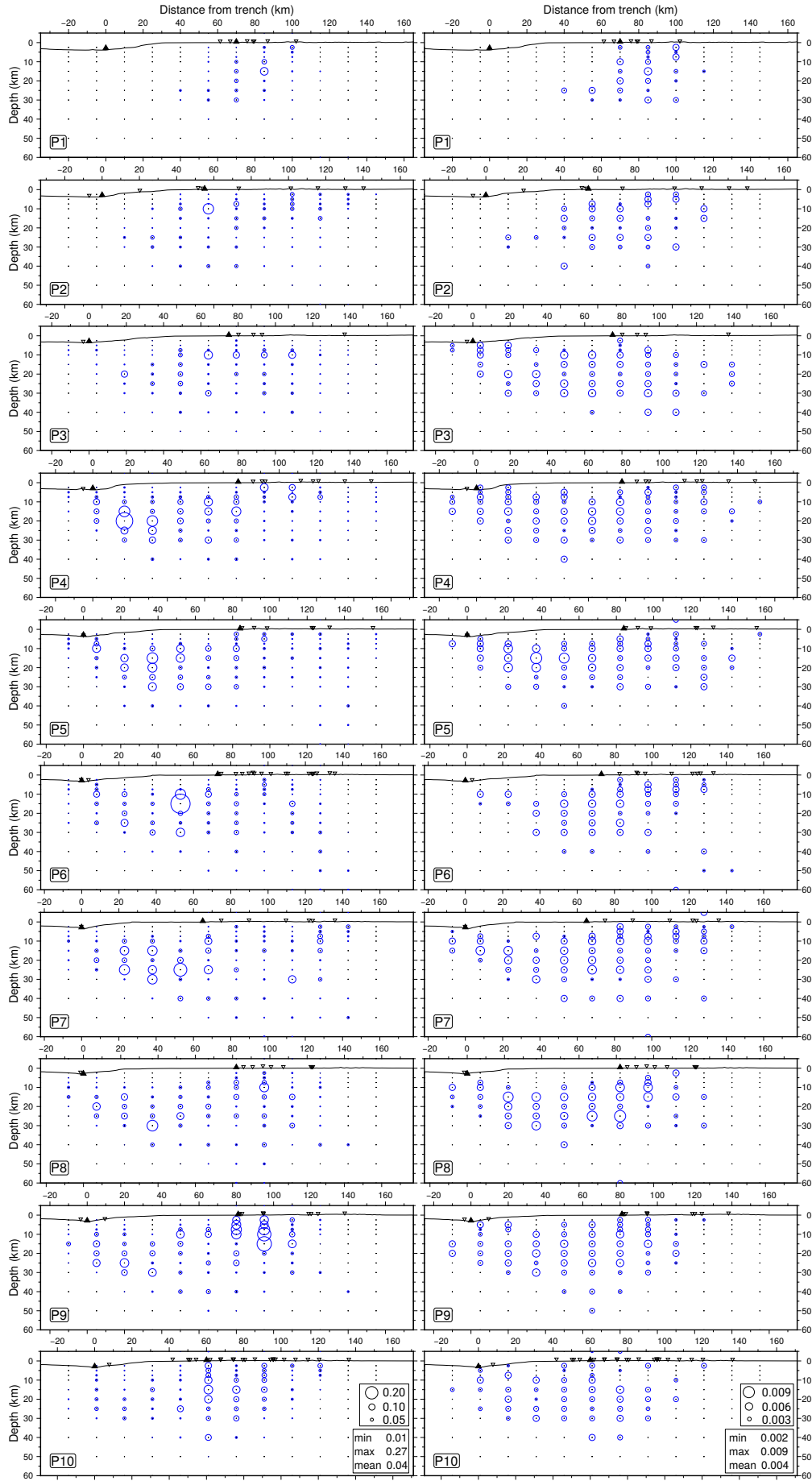


Figure S 9: Estimated Standard deviation. Bootstrap results for an inversion based on a randomly selected subset of aftershocks comprising 80% of the events in our actual catalogue. Blue circles indicate the size of the standard deviation at each profile. (left) V_p , (right) V_p/V_s .

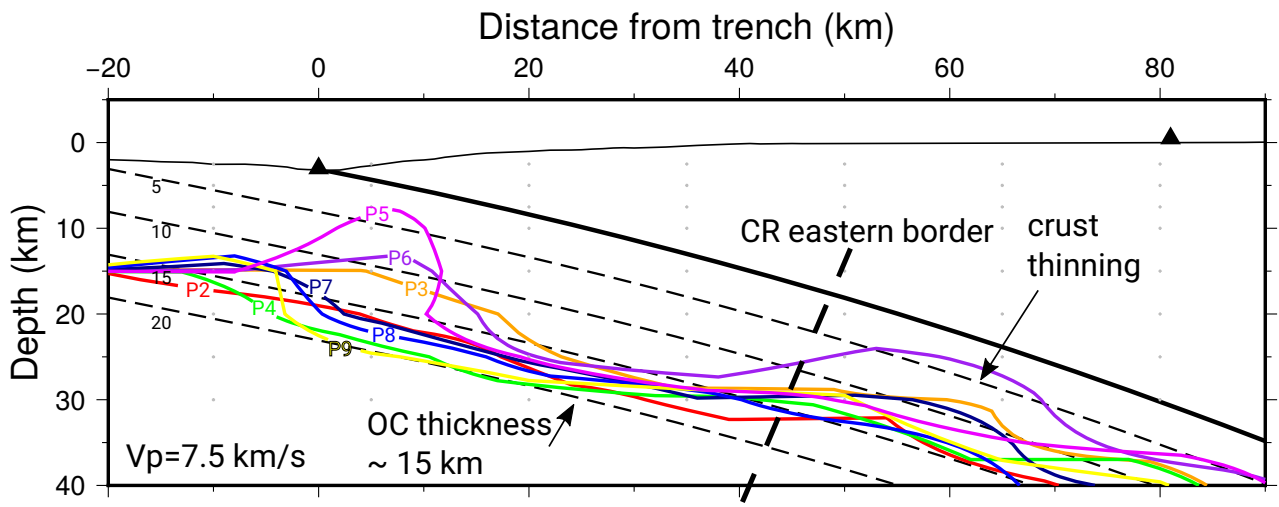


Figure S 10: Analyzing Vp iso-velocity contours. Vp velocities associated to the oceanic upper mantle (bottom). Cross sections compare the depth of profiles P2-P9 identified by colored solid lines. Slab interface and its projection at 5, 10 , 15 and 20 km are plotted for reference. Black triangle represents the trench.

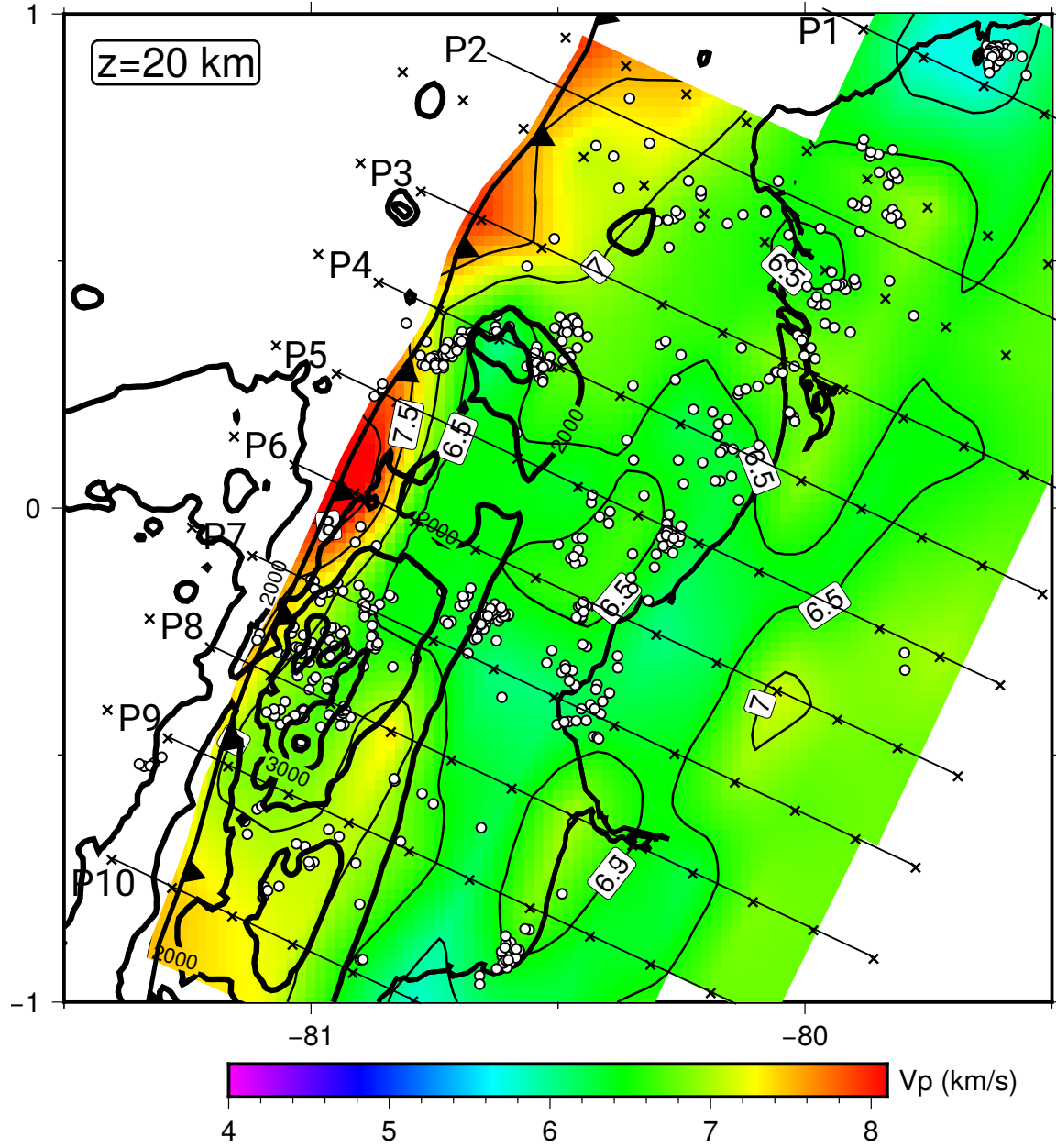


Figure S 11: Constrasting residual bathymetry and V_p horizontal slice. Residual bathymetry derived by Agurto-Detzel et al (2019) superimposed over our 3D V_p velocities obtained for a horizontal slice at 10 km depth.

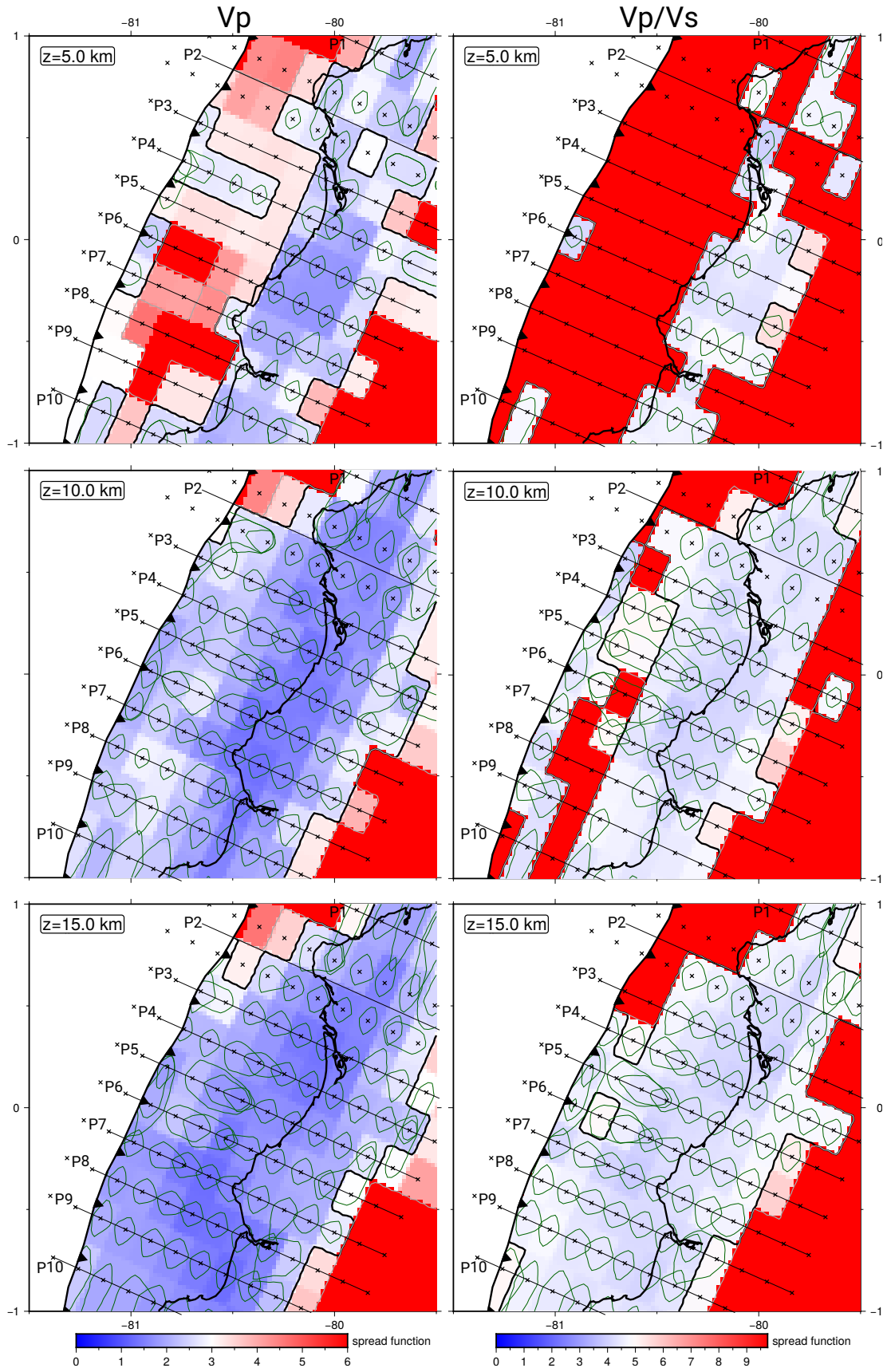


Figure S 12: MRM analysis along strike. Horizontal slices for the obtained 3D Vp (left) and Vp/Vs (right) models at 5, 10 and 15 km depth to estimate the sentivity of the solution along strike.